The Effects of Vinflunine, Vinorelbine, and Vinblastine on Centromere Dynamics[1]

Tatiana Okouneva, Bridget T. Hill, Leslie Wilson, and Mary Ann Jordan[2]

Department of Molecular, Cellular, and Developmental Biology University of California Santa Barbara, Santa Barbara, California 93106 [T. O., L. W., M. A. J.], and Centre de Recherche Pierre Fabre, 81106 Castres Cedex, France [B. T. H.]

Abstract

Vinflunine is a novel fluorinated *Vinca* alkaloid currently in Phase II clinical trials, which in preclinical studies exhibited superior antitumor activity to that of two clinically useful *Vinca* alkaloids, vinorelbine and vinblastine. All three of the drugs block mitosis at the metaphase/anaphase transition, leading to apoptosis. The mechanism of the mitotic block is not known. On the basis of results with purified microtubules and in living interphase cells, we hypothesized that it involves suppression of spindle microtubule dynamics. Here we measured the effects of the three *Vinca* alkaloids on dynamics of centromeres and spindle kinetochore-microtubules by a novel approach involving quantitative time-lapse confocal microscopy in living mitotic human U2OS cells. Green fluorescent protein-labeled centromere-binding protein B was used to mark centromeres and kinetochore-microtubule plus ends. In controls, pairs of centromeres on sister chromatids alternated under tension between increasing and decreasing separation (stretching and relaxing). All three of the *Vinca* alkaloids suppressed centromere dynamics similarly at concentrations that block mitosis. At concentrations approximating the IC_{50}s for mitotic accumulation (18.8 nM vinflunine, 7.3 nM vinorelbine, and 6.1 nM vinblastine), centromere dynamicity decreased by 44%, 25%, and 26%, respectively, and the time centromeres spent in a paused state increased by 63%, 52%, and 36%, respectively. Centromere relaxation rates, stretching durations, and transition frequencies all decreased. Thus all three of the drugs decreased the normal microtubule-dependent spindle tension at the centromeres/kinetochores, thereby preventing the signal for mitotic checkpoint passage. The strong correlation between suppression of kinetochore-microtubule dynamics and mitotic block indicates that the primary mechanism by which the *Vinca* alkaloids block mitosis is suppression of spindle microtubule dynamics.

Introduction

VBL[3] and VNB, antimitotic drugs of the *Vinca* alkaloid class, are widely used in cancer treatment (1). VFL is a new semisynthetic bifluorinated derivative of VNB that is now in Phase II clinical trials (2, 3). In preclinical studies VFL was more effective *in vivo* than VNB or VBL against murine tumors and human tumor xenografts (4–6).

All three of the *Vinca* alkaloids block mitosis at the metaphase/anaphase transition, leading to apoptosis (7–9). We have hypothesized that suppression of microtubule dynamics during mitosis is responsible for the ability of *Vinca* alkaloids to inhibit mitotic progression and cell proliferation. Microtubules are intrinsically dynamic polymers, undergoing two kinds of dynamic behaviors, called dynamic "instability" and "treadmilling." Dynamic instability is the stochastic switching of microtubule ends between episodes of prolonged growing and rapid shortening (10). Treadmilling is net growing at microtubule plus ends and net shortening at minus ends (11–13). Both extensive dynamic instability and treadmilling (or flux) occur in mitotic spindles. The rapid dynamics of spindle microtubules play a critical role in the intricate movements of the chromosomes (14, 15) and may play a crucial role in passage through the metaphase/anaphase checkpoint.

Considerable data have suggested that suppression of microtubule dynamics by *Vinca* alkaloids is responsible for their ability to block mitosis. All three of the *Vinca* alkaloids suppress both microtubule treadmilling and dynamic instability *in vitro* with bovine brain microtubules (7). In addition, in living cells, low concentrations of VBL suppress the growing and shortening dynamics of microtubules during interphase, at the same drug concentrations that block mitosis and inhibit cell proliferation (16). The spindle abnormalities induced by the *Vinca* alkaloids also suggest that the drugs may act to alter microtubule dynamics during mitosis (8). Whereas the *Vinca* alkaloids act specifically during mitosis, it has not been possible to visualize the dynamics of individual microtubules in mitotic cells.

In this work, we used CENP-B labeled with GFP to mark the plus ends of kinetochore-microtubules to analyze the effects of VFL, VNB, and VBL on the dynamics of centromeres, and their attached spindle microtubules during mito-

Received 10/16/02; revised 12/16/02; accepted 2/19/03.
The costs of publication of this article were defrayed in part by the payment of page charges. This article must therefore be hereby marked *advertisement* in accordance with 18 U.S.C. Section 1734 solely to indicate this fact.
[1] Supported by a grant from the Institut de Recherche Pierre Fabre Grant and by USPHS Grant CA57291.
[2] To whom requests for reprints should be addressed, at Department of Molecular, Cellular, and Developmental Biology, University of California Santa Barbara, Santa Barbara, CA 93106. Phone: (805) 893-5317; Fax: (805) 893-4724; E-mail: jordan@lifesci.ucsb.edu.

[3] The abbreviations used are: VBL, vinblastine; VFL, vinflunine; VNB, vinorelbine; CENP-B, centromere-binding protein B; GFP, green fluorescent protein; U2OS, human osteosarcoma cell line.

sis. The kinetochores lie just outside and adjacent to the centromeres, which contain CENP-B. After nuclear envelope breakdown, the microtubules emanating from opposite spindle poles become attached at their plus ends to the centromeres at the kinetochores. These kinetochore-microtubules and their associated motor proteins are responsible for the movements of the chromosomes. During metaphase, before passage through the metaphase-anaphase checkpoint, the two tethered centromeres of each pair of sister chromatids with their attached kinetochore-microtubules alternately stretch apart from each other and return to a relaxed position (17). Elastic heterochromatin between the sister centromeres contains proteins involved in maintaining sister-chromatid cohesion during stretching and relaxing.

We find that all three of the drugs suppress centromere dynamics similarly at the concentrations that block mitosis at the metaphase/anaphase transition. They all markedly decrease overall centromere dynamicity, the rate of relaxation (or coming-together), and the duration of stretching (or pulling apart) of the centromeres. Suppression of the stretching and relaxation movements of the centromeres correlates with mitotic block in a drug concentration-dependent manner, suggesting that suppression of centromere dynamic movement may lead directly to invoking the spindle checkpoint.

Materials and Methods

Cell Culture. U2OS human osteosarcoma cells (American Type Culture Collection, Manassas, VA) were maintained in DMEM supplemented with 1% penicillin-streptomycin, nonessential amino acids (Sigma, St. Louis, MO) and 10% fetal bovine serum (Hyclone, Logan, UT) in 250-ml tissue culture flasks or 35-mm six-well plates (Falcon; Becton Dickinson, Lincoln Park, NJ) at 37°C in a 5% CO_2 atmosphere; their doubling time was 28 h. Cells were transfected with a CENP-B-GFP plasmid containing the coding region for the DNA-binding domain of CENP-B, codons 1–167, fused to the amino terminus of the *Aequorea victoria* GFP cDNA (17). Expression of CENP-B-GFP was stable for 8–10 weeks.

Cell Proliferation and Mitotic Index. Cells were seeded on poly-L-lysine-treated (50 mg/ml, 2 h, 37°C, washed once with sterile water) sterile glass coverslips in six-well plates at 1×10^5 cells/2 ml/well. One day later the medium was replaced with fresh medium containing VFL, VBL, or VNB (1 nM-1 μM), and additionally incubated for one cell cycle (28 h). Cells after such treatment and untreated (control) cells were harvested by combining floating cells with attached cells that had been released by trypsinization [0.5 mg/ml in PBS: 137 mM NaCl, 2.7 mM KCl, 1.5 mM KH_2PO_4, 8.1 mM Na_2HPO_4, and 0.5 mM EDTA (pH 7.2)] for 5 min (37°C), and live cells were counted using a hemacytometer. Trypan blue dye was used to distinguish living from dead cells. Inhibition of cell proliferation was calculated from the difference in cell number for control cultures during the same time period. To evaluate mitotic indices, cells were grown for 20 h in the absence or presence of drug. Mitotic indices were determined by microscopic examination of chromosomes and GFP-CENP-B centromeres in cells that were fixed in formalin/methanol (described below), stained with 4,6-diamidino-2-phenylindole, and imaged using a Nikon Eclipse E800 microscope (Nikon, Melville, NY) with ×60 and ×100 (numerical aperture 1.4 for both) objectives. Results are the mean and SE of four independent experiments in which a minimum of 1000 cells was counted for each condition in each experiment. IC_{50}s were determined by linear regression of double-reciprocal plots of proliferation or mitotic index *versus* drug concentration.

Immunofluorescence Microscopy. Immunofluorescence localization of microtubules and chromosomes was performed on cells that were fixed in 10% formalin in PBS (20 min at 25°C) followed by 10 min in methanol (4°C), washed three times with PBS, and incubated for 30 min with 1% normal donkey serum (Jackson ImmunoResearch Laboratories, Ltd., West Grove, PA) to avoid nonspecific binding. Cells were incubated with rabbit anti-α-tubulin (Cytoskeleton, Denver, CO; 1:1000 dilution) and mouse antihuman histone monoclonal antibodies (Abcam Limited, Cambridge, United Kingdom; 1 h, 37°C). Cells were rinsed three times in PBS containing 1% BSA and incubated with donkey anti-rabbit rhodamine-conjugated secondary antibody and CY5-conjugated antimurine antibody (both from Jackson ImmunoResearch Laboratories, Ltd.; 1:1000 dilution) for 1 h at 37°C. Cells were rinsed three times in PBS-BSA and mounted with VectaShield (Vector, Burlingame, CA). Images were captured with a Nikon Diaphot 200 (Nikon) inverted confocal microscope with a ×100 (numerical aperture 1.4) Nikon PlanApo lens at 3–10% laser power and on a Nikon Eclipse E800 (Nikon) microscope with ×60 and ×100 (numerical aperture 1.4 for both) objectives.

Imaging of Centromeres in Living Cells. After incubation with or without drugs for 4 h to allow attainment of an equilibrium drug concentration in the cells (8), poly-lysine-coated coverslips with live cells attached were mounted in a Dvorak-Stotler chamber (Nicholson Precision Instruments, Gaithersburg, MD) in the medium in which they had been cultured (with or without drug) and maintained on the microscope stage at a temperature of 37°C in a Lucite box. Images of live cells were collected on a Nikon Diaphot 200 inverted confocal microscope with a ×100 Nikon PlanApo lens with a ×7 zoom at 3–10% laser power. Pairs of fluorescent centromeres were easily identified because as the cells enter mitosis, the centromere pairs are oriented perpendicular to the *Z* axis of the microscope. Each time course consisted of a series of 120 single images (2 Kalman images each) taken at 5-s intervals (total time 10 min), at slow scan speed and collected at 128 × 128 pixel box size (each pixel was 0.1 μm). In each time course several centromere pairs could be distinguished and followed.

Image Processing and Quantitative Motility Analysis. Time-lapse image sequences were viewed as movies using Bio-Rad Confocal Assistant Software 4.01 to identify centromere pairs that could be tracked through the sequence for at least 5 min (60 frames). Image stacks were imported into MetaMorph (version 4.0) imaging software (Universal Imaging Corp., Downington, PA) for analysis. The x-y position assigned to a centromere was determined by the brightest pixel at the center of the fluorescent signal and its x-y position, and the distance from the sister centromere was re-

corded on a spreadsheet (Microsoft Excel; Microsoft Corporation, Redmond, WA). Three independent determinations were made of the position of each centromere in each frame of the movie and the results were averaged. The series of separation distances was used to determine rates of separation and relaxing, the durations of these movements, and the frequencies of transition from stretching to relaxing and *vice versa*.

Background Motion. To determine how much of the observed centromere movement was attributable to simple diffusion or to electronic noise rather than to microtubule dynamics and/or motor proteins (which require microtubules for their activity), we measured centromere dynamics in the absence of microtubules. U2OS cells were incubated with 10 μM VBL for 4 h to completely depolymerize all of the microtubules. The mean center-to-center separation between sister centromeres (8 pairs in 4 cells) in the absence of microtubules was 0.58 $\pm$ 0.02 μm, and the average rates of stretching and relaxing were 0.60 $\pm$ 0.01 μm/min and 0.56 $\pm$ 0.02 μm/min, respectively. We determined the total distance that a centromere moved toward and away from its sister for the total time. Mean distance moved plotted against length of interval was 0.34 μm/min. Thus, 0.34 μm/min is the mean rate of movement in the absence of microtubules. Any movement less than or equal to this was considered to be background or diffusional movement and was classified as a "pause."

Criteria for Selection of Centromere Pairs for Measurement of Dynamics. For determination of centromere dynamics, only cells in which the majority of chromosomes had congressed to a well-formed and distinct metaphase plate were measured and only centromere pairs of congressed chromosomes were included. We included only bipolar spindles for measurement in all of the experiments. At high drug concentration (50 nM) ~80% of spindles were bipolar, and many centromeres had not congressed.

Results

Effects of VFL, VNB, and VBL on Mitosis in U2OS Cells. The goal of these experiments was to measure the dynamics of centromeres/kinetochores and their attached microtubules in living U20S cancer cells at the lowest *Vinca* alkaloid concentrations that inhibited proliferation and slowed or blocked mitosis. Thus, we first determined the effects of the drugs on cell proliferation and mitotic progression. Cells were incubated with drug at a range of concentrations (1 nM to 1 μM), and the increase in live cell number during one cell cycle (28 h) was compared with the increase in the absence of drug (Fig. 1*A*). Proliferation was inhibited by 50% at 40 nM VFL, 5.7 nM VNB, and 1.0 nM VBL.

The effects of the three *Vinca* alkaloids on mitotic progression were measured by incubating the cells with a range of drug concentrations (between 1 nM and 330 nM), and determining the mitotic index ("Materials and Methods"). At concentrations of all three drugs >1 nM, cells accumulated in mitosis reaching a maximum accumulation of 38–42% at 100–330 nM drug (Fig. 1*B*). IC_{50} values for mitotic accumulation were 18.8 nM for VFL, 7.3 nM for VNB, and 6.1 nM for VBL. Thus, the primary effects of VFL, VNB, and VBL on

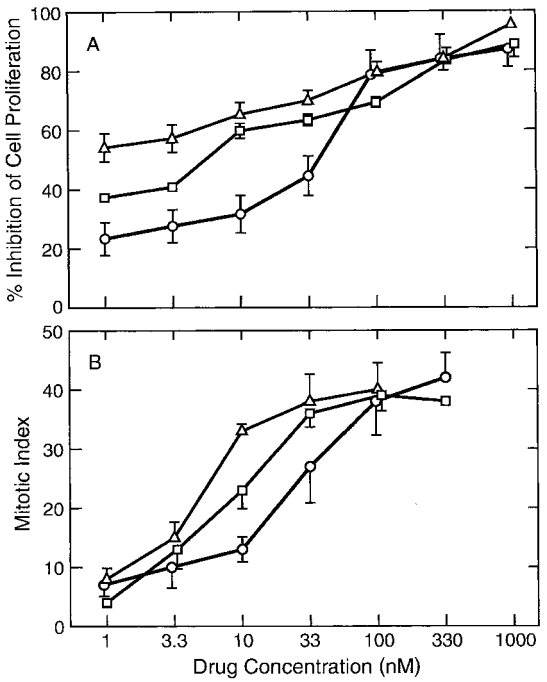

Fig. 1. Concentration dependence for inhibition of proliferation (*A*) and accumulation in mitosis (*B*) of U2OS cells by VFL (○), VNB (□), or VBL (△). Cell proliferation was determined by counting live cells at the time of drug addition and 28 h later. The IC_{50} for inhibition of proliferation for VFL was 40 nM, for VNB was 5.7 nM, and for VBL was <1.0 nM. Accumulation of cells in mitosis was determined by counting cells by immunofluorescence microscopy after fixation and staining of microtubules and chromatin. The IC_{50} for mitotic accumulation for VFL was 18.8 nM, for VNB was 7.3 nM, and for VBL was <6.1 nM. Values are mean of four independent experiments; *bars,* ±SE. Where error bars are not visible, they were smaller than the symbol.

mitosis were detectable over the concentration range of 1–100 nM. We chose to examine centromere dynamics within this range, at two concentrations of VNB and VBL (5 nM and 50 nM) and three concentrations of VFL (5 nM, 18 nM, and 50 nM).

Spindle and Microtubule Organization, and Localization of GFP-CENP-B. The arrangement of GFP-CENP-B, microtubules, and chromosomes in the absence and presence of VFL (4 h incubation) are shown in fixed and immunostained cells in Fig. 2, *A–F*. In untreated cells at metaphase (Fig. 2*A*), chromosomes were completely congressed to the metaphase plate, and all of the centromere pairs were oriented parallel to the spindle axis. The GFP-labeled centromeres appeared as round or elongated green spots of approximately 300–400 nm diameter. During anaphase, sister chromatids and their associated centromeres separated and the centromeres appeared as single, spherical dots (Fig. 2*B*). After incubation with low concentrations of the *Vinca* alkaloids, as shown with 5 nM VFL (Fig. 2*C*) and 18 nM VFL (Fig. 2*D*), a few spindles appeared relatively normal and bipolar with all of the chromosomes congressed to the metaphase plate. GFP-centromere pairs were similar to those in untreated cells, except that they were slightly larger and more diffuse. After incubation with 50 nM VFL, many metaphase

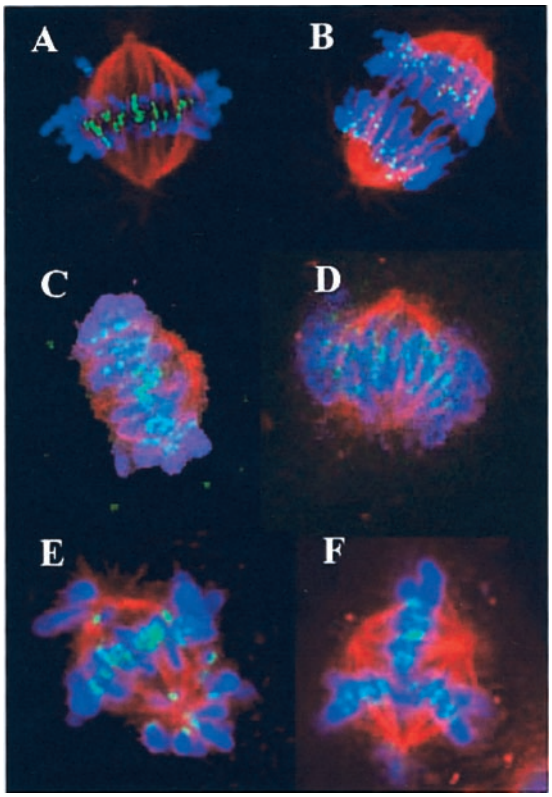

Fig. 2. Centromeres, microtubules, and chromosomes in U2OS cells in the absence (*A* and *B*) or presence (*C–F*) of VFL. Cells expressing GFP-CENP-B were incubated with or without VFL (28 h), fixed, and stained with antibodies to α-tubulin (*red*) and to histone protein (*blue*), and imaged by confocal microscopy ("Materials and Methods"). In untreated cells in metaphase (*A*), pairs of sister centromeres are present on sister chromatids. In untreated cells in anaphase (*B*), sister chromatids and centromeres have separated. In the presence of 5 nM VFL (*C*) or 18 nM VFL (*D*), some spindles appeared relatively normal with the exception that centromeres were more diffuse and larger than in untreated cells. Some spindles had a few or many chromosomes that had not congressed and remained at one of the poles (*E*, 50 nM VFL), and some were tripolar with three plates of congressed chromosomes (*F*, 50 nM VFL).

cells had one or more chromosomes that remained uncongressed and were located at one or both spindle poles (Fig. 2*E*), and some spindles were tripolar or multipolar (VFL, 19.8 ± 4.3%; VNB, 18.3 ± 5.1%; VBL, 23.6 ± 4.8%; Fig. 2*F*).

Centromere Dynamics in the Absence of Drugs. The sister centromeres of each chromatid pair alternated between phases of increasing and decreasing separation; *i.e.,* they alternately stretched apart and relaxed back together. The behavior of a typical pair of centromeres in an untreated cell during a 480-s period is shown in Fig. 3, *A–E*. In Fig. 3*A,* at time 0, the sister centromeres (arrows) were separated by 0.4 μm. In Fig. 3, *B–D* (at 120, 240, and 360 s), they were separated by 0.6, 0.8, and 1 μm, respectively. In Fig. 3*E* (480 s), they had relaxed back together and were only 0.5 μm apart. The stretching and relaxing movements of each centromere pair were independent of the movements of other centromere pairs in the same cell (Fig. 3).

Fig. 4 shows a time course of the stretching and relaxing movements of two pairs of sister centromeres determined from images like those in Fig. 3. The panels represent the distance between the two centromeres of a pair in an untreated cell (A) and in the presence of 50 nM VFL (B). These plots, which are analogous to "life history" plots of microtubule growth and shortening dynamics (*e.g.*, see Ref. 18), were used to determine the parameters of sister centromere dynamics. The members of the lower pair of sister centromeres (in the presence of 50 nM VFL) were closer together on average. Both the frequency and amplitude of their separation movements were reduced as compared with centromeres in untreated cells.

As shown in Figs. 5 and 6, pairs of sister centromeres in untreated cells stretched at a mean rate of 1.0 ± 0.4 μm/min for 13.1 ± 2.5 s to a mean maximal separation distance of 0.94 ± 0.07 μm, and they relaxed at a mean rate of 1.5 ± 0.4 μm/min for 11.8 ± 2.8 s to a mean minimal separation distance of 0.47 ± 0.09 μm. Overall, centromere pairs in control cells spent 36.1 ± 1.4% of the time stretching, 32.4 ± 1.6% relaxing, and 31.6 ± 2.4% in a paused phase in which their movements could not be clearly distinguished from the movements that occurred in the absence of attached microtubules (Fig. 7). They transitioned between stretching and relaxing 1.7 times per min (Fig. 8*B*). We also calculated the overall rate of centromere stretching and relaxation movement, which we call the "centromere dynamicity," analogous to the term used to describe overall microtubule dynamics (19). In this situation, dynamicity consists of the sum of the distances moved during stretching and relaxation divided by the total time measured. The mean centromere dynamicity in the absence of drugs was 0.84 μm/min (Fig. 8*A*).

VFL, VNB, and VBL All Suppressed Centromere Dynamics, with Only Small Differences in the Altered Parameters among the Three Drugs. Cells were incubated with each *Vinca* alkaloid for 4 h before measuring centromere dynamics, because uptake of these drugs into cells reaches equilibrium in ~4 h (8). From the data presented in Figs. 6–8, it is evident that, in general, all three of the *Vinca* alkaloids suppressed centromere dynamics over the concentration range that blocked mitosis and inhibited cell proliferation (5–50 nM). The suppressive effects increased with increasing drug concentration in this range. For example, as shown diagrammatically in Fig. 5 for 50 nM VFL, the rate of stretching decreased only slightly (by 10%), but significantly, from 1.0 ± 0.4 μm/min in controls to 0.9 ± 0.1 μm/min at 50 nM VFL, whereas the rate of relaxation decreased significantly and strongly (by 54%), from 1.5 ± 0.4 μm/min in controls to 0.7 ± 0.2 μm/min. The durations of stretching and relaxation were both reduced strongly and significantly by 50 nM VFL (Figs. 5 and 6). VNB and VBL suppressed stretching and relaxation similarly to VFL with the exception that VNB had little effect on the duration of stretching (Fig. 6).

The intercentromere distance is an indicator of tension on centromeres (20). Interestingly, 5 nM VFL (a concentration that did not induce mitotic block), increased the mean intercentromere distance by 31%, from 0.68 ± 0.09 μm in controls to 0.89 ± 0.09 μm (Fig. 9), suggesting that this low VFL concentration actually increased tension. At 18 nM VFL the distance was almost equal to that in controls, and at 50 nM VFL it was reduced by 13% to 0.59 μm (Fig. 9) indicating that

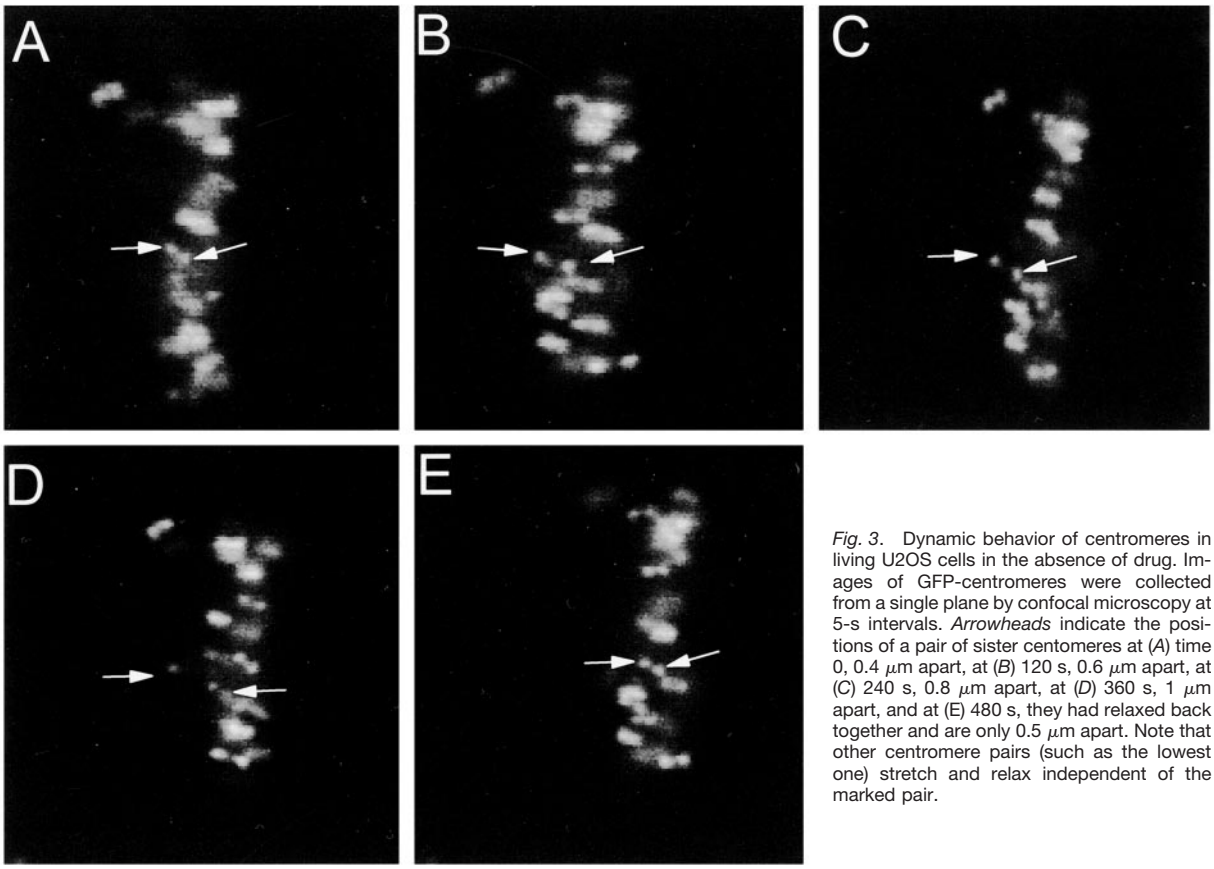

Fig. 3. Dynamic behavior of centromeres in living U2OS cells in the absence of drug. Images of GFP-centromeres were collected from a single plane by confocal microscopy at 5-s intervals. *Arrowheads* indicate the positions of a pair of sister centomeres at (*A*) time 0, 0.4 μm apart, at (*B*) 120 s, 0.6 μm apart, at (*C*) 240 s, 0.8 μm apart, at (*D*) 360 s, 1 μm apart, and at (E) 480 s, they had relaxed back together and are only 0.5 μm apart. Note that other centromere pairs (such as the lowest one) stretch and relax independent of the marked pair.

50 nM VFL reduced tension. We also calculated the mean maximal and mean minimal separation distances for each centromere pair ("Materials and Methods") and found that, as with the mean separation distance, these distances were increased by 5 nM VFL (Fig. 9). At 5 nM VNB and VBL (concentrations that induced mitotic block), the mean separation distance was not appreciably altered (by only 4–7%), but at 50 nM VBL it was strongly reduced (by 40%). Interestingly, all of the concentrations of the three *Vinca* alkaloids significantly increased the minimal separation distance except for 50 nM VBL (Fig. 9).

The time stretching and relaxing decreased by approximately half at 50 nM VFL, and, correspondingly, the time paused more than doubled (Fig. 7). VBL had similar strong effects on the amounts of time spent stretching, relaxing, and paused (increasing the amount of time paused by 146%), but VNB had much less effect on the percentages of time spent stretching, relaxing, and paused (increasing the amount of time paused by only 59%; Fig. 7).

Which Effects of the Drugs on Centromere Dynamics Might Be Responsible for Blocking Mitosis? The most prominent effects of all three of the drugs were on the overall dynamicity, the transition frequencies, and the percentages of time spent in the stretching, relaxation, and pause phases (Table 1; Figs. 7 and 8). For example, at the concentrations closest to the IC_{50}s for mitotic arrest (18 nM VFL, 5 nM VNB, and 5 nM VBL), the three drugs reduced the dynamicity by 44%, 25%, and 26%, they increased the time spent paused by 63%, 52%, and 36%, and they reduced the transition frequencies by 25%, 14%, and 27%, respectively.

The rate of relaxation was also prominently suppressed at the IC_{50} values of the three drugs (by 32%, 24%, and 41%, for 18 nM VFL, 5 nM VNB, and 5 nM VBL, respectively), but the durations of relaxation were almost unchanged (Table 1; Fig. 6). Relaxation is a result of microtubule growth (see "Discussion"); thus, suppression of the relaxation rate is likely to result from suppression of microtubule growth by the drugs. Similarly, stretching is likely to result, at least in part, from microtubule shortening. The stretching rate was relatively unchanged by VFL, but it was increased at the IC_{50}s for VNB and VBL (by 32% and 21%, respectively; Table 1; Fig. 6). The duration of stretching was suppressed to some extent (by 19%, 15%, and 11%) at the IC_{50}s for VFL, VNB, and VBL, respectively).

It is noticeable that change in the mean separation distance (Table 1; Fig. 9) was small for all three of the drugs at their IC_{50}s, but additional analysis of the data (see "Discussion") indicates that the separation distance may contribute importantly to signaling passage through the metaphase/anaphase checkpoint.

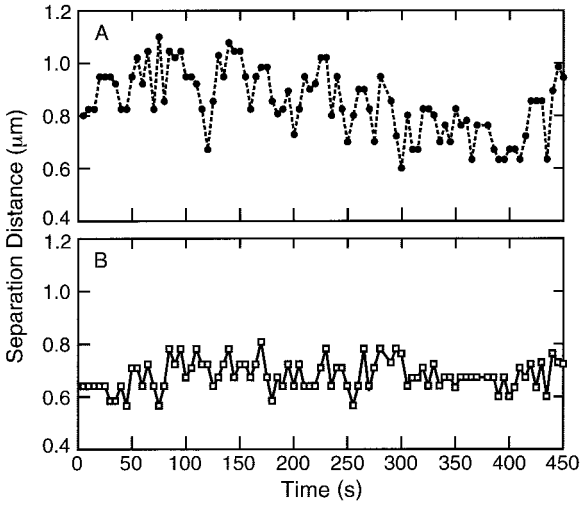

Fig. 4. Time course of changes in the center-to-center separation distance between a pair of sister centromeres in the absence of drug (*top trace*) and in the presence of 50 nM VFL (*bottom trace*). Images of GFP centromeres were collected from a single plane by confocal microscopy at 5-s intervals. Separation distances between the two members of pairs were measured as described in "Materials and Methods." The separation between the members of a pair alternated between episodes of stretching and episodes of relaxing. For example, at time 0, in the absence of drug, the pair was separated by 0.80 μm. At 300 s, the pair was separated by 0.60 μm (the minimal separation observed for this pair), and at 450 s the separation was increased to 0.98 μm. The maximal separation observed for this pair was 1.15 μm at 75 s. In the presence of 50 nM VFL, the separation distance was reduced overall, and ranged from 0.81 to 0.56 μm in this trace. For some periods, for example, from 340 to 425 s, pairs remained in a phase of little or no detectable change in separation distance called a "pause."

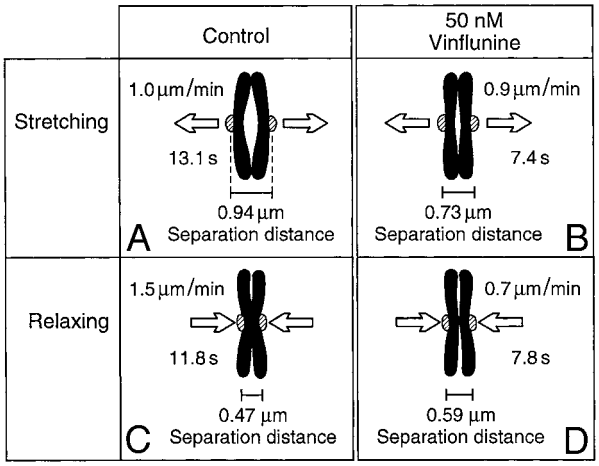

Fig. 5. Diagram showing an average stretching event in the absence of drug (*A*) and in the presence of 50 nM VFL (*B*). The means, rates, durations, and mean maximal and minimal separation distances are indicated on each panel. Centromeres stretched farther apart and for longer time in the absence of drug. *Bottom row* (*C* and *D*) shows a typical relaxation event −/+ VFL. Centromeres relaxed together faster and for longer time periods in the absence of drug.

Discussion

During metaphase, chromosome pairs oscillate toward and away from the spindle poles, independent of neighboring chromosomes, as the attached kinetochore-microtubules periodically grow and shorten (21, 22). Shortening and growth of the kinetochore-microtubules, together with the actions of mitotic motors, result in separation (stretching) and coming together (relaxation) of sister centromeres. Using GFP-CENP-B to mark the ends of the microtubule-tethered-kinetochores, we analyzed the effects of VFL, VNB, and VBL on centromere and kinetochore-microtubule dynamics in living mitotic cells. In general, at the IC_{50}s for mitotic block, the three *Vinca* alkaloids affected centromere dynamics similarly. They markedly decreased centromere dynamicity, primarily by increasing the time centromeres remained in a paused state. For example, at the IC_{50}s for mitotic accumulation (~18 nM for VFL, 5 nM for VNB, and 5 nM for VBL), centromere dynamicity was reduced by 44%, 25%, and 26%, respectively, and the amount of time the centromere pairs remained in a paused state increased by 63%, 52%, and 36%, respectively (Table 1). In addition, at their IC_{50}s the three drugs all suppressed the relaxation rate, decreased the stretching duration, and decreased the transition frequencies. They did not greatly or consistently alter the stretching rate or the relaxation duration. In addition, the drugs induced relatively small changes in the mean separation distance. Suppression of the stretching and relaxation movements correlated strongly with inhibition of mitosis at prometaphase/metaphase suggesting that suppression of centromere dynamic movements is important in the metaphase/anaphase checkpoint.

The Spindle Checkpoint and Spindle Tension. The metaphase checkpoint ensures that chromosomes properly attach to the mitotic spindle and align at the metaphase plate before anaphase onset. Passage through the checkpoint appears to depend on tension at the kinetochores and/or on occupancy of the kinetochores by a sufficient number of microtubules (22–24). Whereas all three of the *Vinca* alkaloids affected specific dynamics parameters somewhat differently, they all reduced centromere dynamicity significantly, and to similar degrees, at the concentrations that induced mitotic accumulation suggesting that the important parameters resulting in mitotic block are those of which the combined effects reduce tension at the kinetochores.

Cell Cycle Progression at the Mitotic Checkpoint Is Sensitive to Moderate Suppression of Centromere Dynamics. Fifty nM VNB induced maximal mitotic block in U2OS cells; yet, at this concentration there was only minimal or moderate suppression of many of the parameters of centromere dynamics (Figs. 6–9). Fifty nM VNB induced only 18% reduction in the rate of stretching, 38% reduction in the rate of relaxation, 4% reduction in the mean separation, 44% reduction in the transition frequency, and 46% reduction in dynamicity. Thus, such changes appear to be sufficient to nearly completely inhibit the transition from metaphase into anaphase.

The Effects of the *Vinca* Alkaloids on Centromere Dynamics Correlate Well with Their Effects on Microtubule Dynamics *in Vitro*. We found previously that the major effects of VFL and VNB on dynamic instability of microtubules assembled from purified brain tubulin *in vitro* differed significantly from those of VBL. The two newer *Vinca* alkaloids

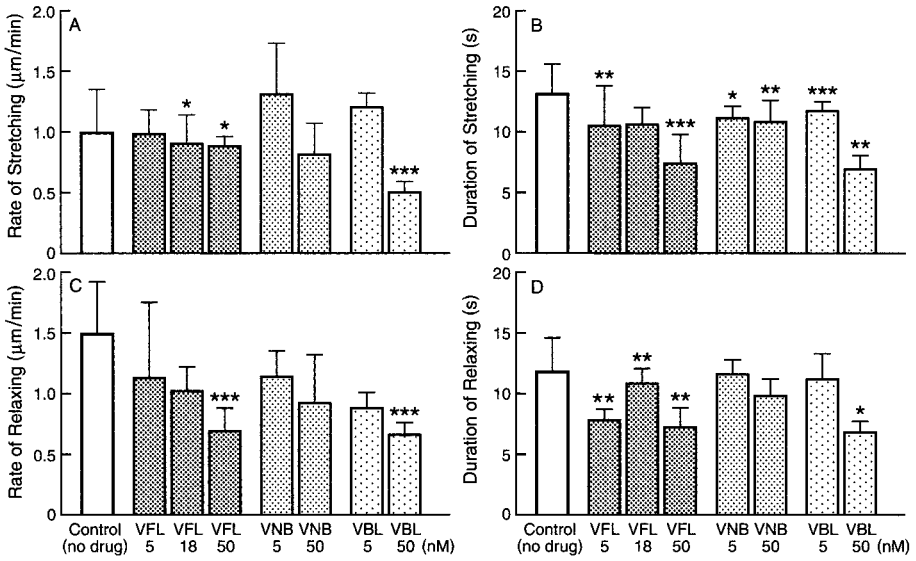

Fig. 6. Effects of *Vinca* alkaloids on the rates of stretching (*A*) and relaxing (*C*), and the duration of stretching (*B*) and relaxing (*D*). *Bars,* ±SE. Between 6 and 11 pairs of centromeres from between 7 and 14 cells were measured for each condition. *, **, *** values were significantly different from control values with $P < 0.05$, $P < 0.01$, and $P < 0.001$, respectively (Student's *t* test).

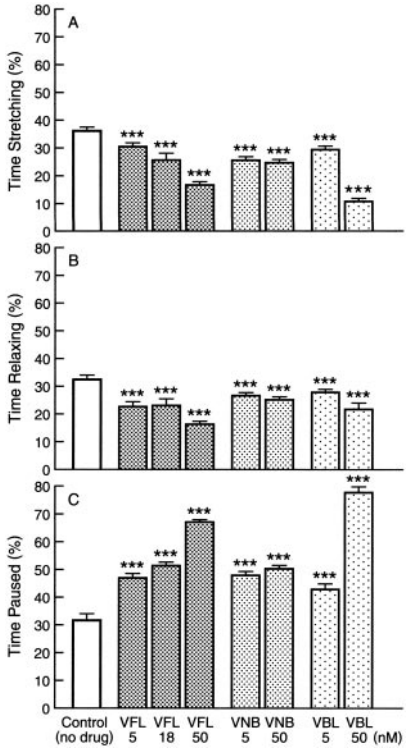

Fig. 7. Effects of *Vinca* alkaloids on the amount of time spent in stretching (*A*), relaxing (*B*), and paused (*C*). *Bars,* ±SE. *, **, *** values were significantly different from control values with $P < 0.05$, $P < 0.01$, and $P < 0.001$, respectively (Student's *t* test).

slowed growth rates, increased growth durations, and reduced shortening durations but in contrast with VBL, did not reduce shortening rates or increase the percentage of time the microtubules spent in an attenuated state (7). The differential effects of the three drugs on microtubule shortening rates *in vitro* correlate well with their effects on centromere stretching rates. The stretching rate must reflect the shortening rate of the kinetochore-attached microtubules. In mitotic cells, 50 nM VFL or VNB only minimally reduced the stretching rate (by 11–18%; Fig. 6). Similarly, 400 nM VFL or VNB did not affect the microtubule shortening rate *in vitro*. In contrast, 400 nM VBL strongly reduced the shortening rate *in vitro* (by 44%; Ref. 7) and 50 nM VBL reduced the stretching rate by 49% (Fig. 6). Centromere stretching may also involve tension exerted on the centromere pairs by poleward treadmilling or flux of the kinetochore microtubules. VBL inhibits the rate of treadmilling 7 times more strongly than VNB and 28 times more strongly than VFL (7). Thus, the effects of the three drugs on centromere stretching in living cells correlate well with their inhibitory effects both on microtubule treadmilling and dynamic instability *in vitro*.

It is likely that centromere relaxation involves the kinetochore-microtubules growing toward and pushing against the centromeres (21). Microtubule growing rates *in vitro* and centromere relaxation rates in mitotic cells were suppressed similarly by all three of the *Vinca* alkaloids (Ref. 7; Fig. 6).

Interestingly, the differences between the effects of the *Vinca* alkaloids on the durations of microtubule growth and shortening excursions observed previously *in vitro* (7) did not correlate with the durations of centromere stretching and relaxation excursions in cells. Specifically, 400 nM VFL and VNB increased the growth duration *in vitro* by >50%, but 400 nM VBL had little effect on it (7). Similarly, VFL and VNB reduced the shortening duration *in vitro*, but VBL increased it (7). In contrast, VFL and VBL affected the durations of relaxing and stretching similarly in cells, whereas VNB had little effect (Fig. 6). This lack of correlation is perhaps not surprising. *In vitro*, the microtubule plus ends are unconstrained and transition freely between phases of growth and shortening. However, in cells, the plus ends of kinetochore-microtubules are constrained because they are tethered at the kinetochores (22) and because they are connected to the opposite microtubule bundle through the elastic α-satellite DNA that connects the sister chromatids. Thus, the durations of the

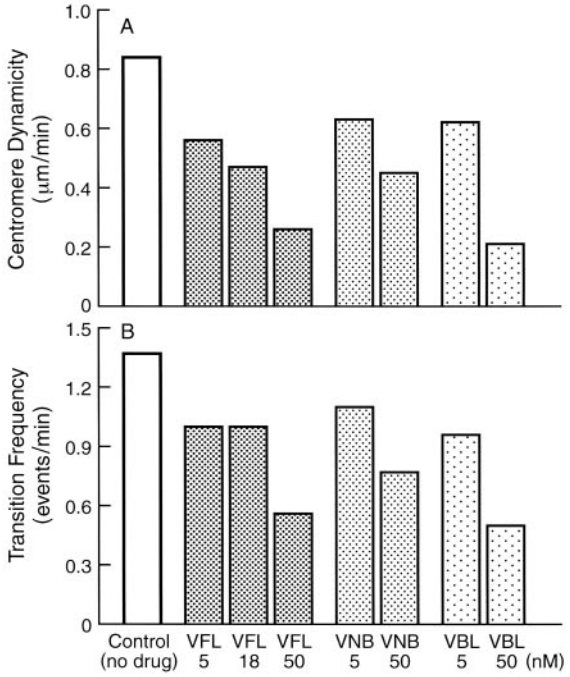

Fig. 8. Effects of VFL, VNB, and VBL on overall dynamicity, and on the frequency of transition between phases of stretching and relaxing.

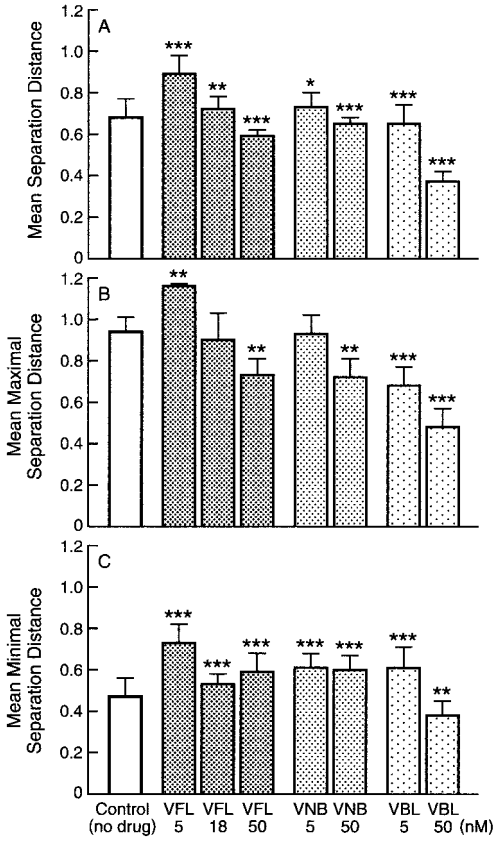

Fig. 9. Effects of *Vinca* alkaloids on the mean separation distance between centromeres of a pair (*A*), their maximal separation distance (*B*), and their minimal separation distance (*C*; "Materials and Methods"). *Bars,* ±SE. *B* and *C* are the mean for all tracings of the two maximal separations (*B, peaks*) or the two minimal separations (*C, valleys*) during each 5-min tracing for each condition. The mean separation distance in the absence of microtubules (after incubation with 10 μM VBL) was 0.58 ± 0.02 μm. *, **, *** values were significantly different from control values with $P < 0.05$, $P < 0.01$, and $P < 0.001$, respectively (Student's *t* test).

centromere stretching and relaxation movements are probably determined by external factors and may not be as susceptible to drug action as microtubules *in vitro*.

At first glance, it may appear contradictory that the magnitude of the effects of the *Vinca* alkaloids at a concentration of 400 nM on microtubule dynamicity *in vitro* (suppression by 21% to 32%) were weaker than that exerted by a concentration of 50 nM on centromere dynamicity (suppression by 46% to 75%). However, this is readily explained, because *Vinca* alkaloids are concentrated between 130- and 430-fold in cells (8). Thus, it is likely that in U2OS cells the intracellular concentrations of the drugs after incubation with 50 nM drug were significantly higher than the 400 nM drug used *in vitro*.

Why Does VFL Inhibit Cell Proliferation and Block Mitosis Less Potently Than VNB or VBL? VNB and VBL reduced cell proliferation by 50% at concentrations of 5.7 nM and 1.0 nM, respectively, whereas VFL was significantly less potent (IC_{50}, 40 nM). Similarly, the IC_{50}s for mitotic accumulation induced by the drugs also differed significantly, with the IC_{50} of VFL (18.8 nM) being much higher than those of VNB (7.3 nM) and VBL (6.1 nM). Therefore, it is surprising that many of the centromere dynamics parameters were affected similarly by similar concentrations of the three drugs. The principal exception was the centromere separation distance, which reflects the amount of tension exerted by the two tethered kinetochores. At 5 nM VFL the mean, maximal, and minimal separation distances were all increased significantly, indicating that VFL significantly increases tension. In contrast, 5 nM VNB or VBL had little effect on the separation distance. Thus, 5 nM VFL increased the tension on the kinetochore proteins, which would be predicted to facilitate passage through the mitotic checkpoint, as was observed. On the other hand, VNB and VBL had little or opposite effects, consistent with a reduction of tension and their increased ability to block mitosis. These data support the hypothesis that the centromere separation distance may play an important role in determining passage through the metaphase/anaphase checkpoint.

We note that the relationship between the IC_{50}s for inhibition of proliferation and for mitotic block differ for the three drugs. Thus, the IC_{50} for mitotic accumulation is half the IC_{50} for inhibition of proliferation for VFL, equal to the IC_{50} for VNB, and 6-fold higher for VBL. This relationship suggests that interesting differences exist among the drugs in the permanence of the mitotic block they produce.

Why Does 5 nM VFL Increase the Intercentromere Distance? What Is the Role of Motor Proteins in Centromere Dynamics? The magnitude of the intercentromere distance must depend, in part, on microtubule shortening and/or treadmilling, and/or motor proteins. VFL suppresses treadmilling *in vitro* significantly less potently than VNB or VBL (7); this difference may be responsible for its inability to

Table 1 Percentage change in parameters of centromere dynamics induced by the IC_{50}s for mitotic block by VFL, VNB, and VBL in U2OS cells as compared with untreated cells

Parameter	18 nM VFL, % change	5 nM VNB, % change	5 nM VBL, % change
Mean separation distance	5.9	7.4	−4.4
Maximal separation distance	−4.3	−1.1	−27.7
Minimal separation distance	13	30	30
Stretching rate	−9.1	32	21
Relaxing rate	−32	−24	−41
Stretching duration	−19	−15	−11
Relaxing duration	−8.3	−1.7	−5.0
% Time stretching	−29	−29	−19
% Time relaxing	−29	−18	−14
% Time paused	63	52	36
Transition frequency	−25	−14	−27
Dynamicity	−44	−25	−26

suppress the intercentromere stretching distance at 5 nM drug. The affinities of the three drugs for tubulin differ, and VFL has fewer binding sites on tubulin than VNB, indicating that a clear difference exists in the interactions of these *Vinca* alkaloids with tubulin (25–28). The increased intercentromere distance induced by 5 nM VFL may result from complex interactions between the drug and kinetochore motor proteins, as well as through differential drug effects at both microtubule ends (29). The lack of a strong suppression of centromere dynamics by 5 nM VFL might facilitate the activity of motors acting at the microtubule surface, perhaps leading to a motor-driven increase in the intercentromere distance.

Taken together, the data show that reduced tension on kinetochores/centromeres as a result of suppression of microtubule dynamics by the *Vinca* alkaloids plays a major role in their ability to block mitosis and inhibit tumor cell growth. The results, as well as similar results with taxol (30), indicate a central role for microtubule treadmilling and dynamic instability in regulating cell cycle progression through the spindle checkpoint.

Acknowledgments

We thank Dr. Kevin Sullivan for the gift of GFP-CENP-B-transfected U2OS cells and Kathryn Kamath for critical reading of the manuscript.

References

1. Kruczynski, A., and Hill, B. T. Vinflunine, the latest Vinca alkaloid in clinical development. A review of its preclinical anticancer properties. Crit. Rev. Oncol.-Hematol., *40:* 159–173, 2001.

2. Armand, J. P., Fumoleau, P., Marty, M., Variol, P., Pinel, M. C., Picard, M., and Puozzo, C. Pharmacokinetics of vinflunine, a novel Vinca alkaloid, during the Phase I does escalation study (D1 Q 3 WEEKS). Proc. Am. Assoc. Cancer Res., 381, 2001.

3. Fumoleau, P., Raymond, E., Bennouna, J., Armand, J-P., Hocini, A., Blanchot, G., Pinel, M., De Bie, J., and Marty, M. Phase I trial of vinflunine (L0070), a novel fluorinated Vinca alkaloid in patients (pts) with advanced solid malignancies: final results. Proc. Am Assoc. Cancer Res, *42:* 834, 2001.

4. Hill, B., Fiebig, H., Waud, W., Poupon, M., Colpaert, F., and Kruczynski, A. Superior *in vivo* experimental antitumour activity of vinflunine, relative to vinorelbine, in a panel of human tumour xenografts. Eur. J. Cancer, *35:* 512–520, 1999.

5. Kruczynski, A., Colpaert, F., Tarayre, J., Mouillard, P., Fahy, J., and Hill, B. Preclinical *in vivo* antitumor activity of vinflunine, a novel fluorinated Vinca alkaloid. Cancer Chemother. Pharmacol., *41:* 437–447, 1998.

6. Kruczynski, A., Barret, J-M., Etievant, C., Colpaert, F., Fahy, J., and Hill, B. T. Antimitotic and tubulin interacting properties of vinflunine, a novel fluorinated Vinca alkaloid. Biochem. Pharmacol., *55:* 635–648, 1998.

7. Ngan, V. K., Bellman, K., Panda, D., Hill, B. T., Jordan, M. A., and Wilson, L. Novel actions of the antitumor drugs vinflunine and vinorelbine on microtubules. Cancer Res., *60:* 5045–5051, 2000.

8. Ngan, V., Bellman, K., Hill, B., Wilson, L., and Jordan, M. Mechanism of mitotic block and inhibition of cell proliferation by the semisynthetic Vinca alkaloids vinorelbine and its newer derivative vinflunine. Mol. Pharmacol., *60:* 225–232, 2001.

9. Kruczynski, A., Etievant, C., Perrin, D., Chansard, N., Duflos, A., and Hill, B. T. Characterization of cell death induced by vinflunine, the most recent Vinca alkaloid in clinical development. Br. J. Cancer *86*: 143–150, 2002.

10. Mitchison, T. J., and Kirschner, M. Dynamic instability of microtubule growth. Nature (Lond.), *312:* 237–242, 1984b.

11. Margolis, R. L., and Wilson, L. Microtubule treadmilling: What goes around comes around. Bioessays, *20:* 830–836, 1998.

12. Rodionov, V. I., Nadezhdina, E., and Borisy, G. G. Centrosomal control of microtubule dynamics. Proc. Natl. Acad. Sci. USA, *96:* 115–120, 1999.

13. Panda, D., Miller, H. P., and Wilson, L. Rapid treadmilling of brain microtubules free of microtubule-associated proteins *in vitro* and its suppression by tau. Proc. Natl. Acad. Sci. USA, *96*: 12459–12464, 1999.

14. Mitchison, T. J. Poleward microtubule flux in the mitotic spindle; evidence from photoactivation of fluorescence. J. Cell Biol., *109:* 637–652, 1989.

15. Hayden, J. J., Bowser, S. S., and Rieder, C. Kinetochores capture astral microtubules during chromosome attachment to the mitotic spindle: direct visualization in live newt cells. J. Cell Biol., *111:* 1039–1045, 1990.

16. Dhamodharan, R. I., Jordan, M. A., Thrower, D., Wilson, L., and Wadsworth, P. Vinblastine suppresses dynamics of individual microtubules in living cells. Mol. Biol. Cell, *6:* 1215–1229, 1995.

17. Shelby, R. D., Hahn, K. M., and Sullivan, K. F. Dynamic elastic behavior of α-satellite DNA domains visualized *in situ* in living human cells. J. Cell Biol., *135:* 545–557, 1996.

18. Yvon, A-M., Wadsworth, P., and Jordan, M. A. Taxol suppresses dynamics of individual microtubules in living human tumor cells. Mol. Biol. Cell, *10:* 947–949, 1999.

19. Toso, R. J., Jordan, M. A., Farrell, K. W., Matsumoto, B., and Wilson, L. Kinetic stabilization of microtubule dynamic instability *in vitro* by vinblastine. Biochemistry, *32:* 1285–1293, 1993.

20. Waters, J. C., Skibbens, R. V., and Salmon, E. D. Oscillating mitotic newt lung cell kinetochores are, on average, under tension and rarely push. J. Cell Sci., *109:* 2823–2831, 1996.

21. Skibbens, R. V., Skeen, V. P., and Salmon, E. D. Directional instability of kinetochore motility during chromosome congression and segregation in mitotic newt lung cells: a push-pull mechanism. J. Cell Biol., *122:* 859–875, 1993.

22. McIntosh, J., Grishchuk, E. L., and West, R. R. Chromosome-microtubule interactions during mitosis. Annu. Rev. Cell Dev. Biol., *18:* 193–219, 2002.

23. Nicklas, R. B., Waters, J. C., Salmon, E. D., and Ward, S. C. Checkpoint signals in grasshopper meiosis are sensitive to microtubule attachment, but tension is still essential. J. Cell Sci., *114:* 4173–4183, 2001.

24. Skoufias, D. A., Andreassen, P., Lacroix, F., Wilson, L., and Margolis, R. L. Mammalian mad2 and bub1/bubR1 recognize distinct spindle-

attachment and kinetochore-tension checkpoints. Proc. Natl. Acad. Sci. USA, *10:* 4492–4497, 2001.

25. Lobert, S., Vulevic, B., and Correia, J. Interaction of vinca alkaloids with tubulin: a comparison of vinblastine, vincristine, and vinorelbine. Biochemistry, *35:* 6806–6814, 1996.

26. Lobert, S., Ingram, J., Hill, B., and Correia, J. A comparison of thermodynamic parameters for vinorelbine- and vinflunine-induced tubulin self-association by sedimentation velocity. Mol. Pharmacol., *53:* 908–915, 1998.

27. Fabre, C., Czaplicki, J., Wright, M., Hill, B., Barret, J., Fahy, J., and Milon, A. Differential binding to the α/β-tubulin dimer of vinorelbine and vinflunine revealed by nuclear magnetic resonance analyses. Biochem. Pharmacol. *64*: 733, 2002.

28. Jordan, M. A. Mechanism of action of antitumor drugs that interact with microtubules and tubulin. Curr. Med. Chem.–Anti-Cancer Agents, *2:* 1–17, 2002.

29. Panda, D., Jordan, M. A., Chin, K., and Wilson, L. Differential effects of vinblastine on polymerization and dynamics at opposite microtubule ends. J. Biol. Chem., *271:* 29807–29812, 1996.

30. Kelling, J., Sullivan, K., Wilson, L., and Jordan, M. A. Suppression of centromere dynamics by taxol in living osteosarcoma cells. Cancer Res. *63:* in press, 2003.

Molecular Cancer Therapeutics

The Effects of Vinflunine, Vinorelbine, and Vinblastine on Centromere Dynamics [1]

Tatiana Okouneva, Bridget T. Hill, Leslie Wilson, et al.

Mol Cancer Ther 2003;2:427-436.